Monographs in Electrochemistry
Series Editor: F. Scholz

Oscar Alejandro Oviedo
Luis Reinaudi
Silvana Graciela García
Ezequiel Pedro Marcos Leiva

Underpotential Deposition

From Fundamentals and Theory to Applications at the Nanoscale

Springer

Underpotential Deposition

Monographs in Electrochemistry

Series Editor: Fritz Scholz, University of Greifswald, Germany

Surprisingly, a large number of important topics in electrochemistry are not covered by up-to-date monographs and series on the market, some topics are even not covered at all. The new series "Monographs in Electrochemistry" will fill this gap by publishing in-depth monographs written by experienced and distinguished electrochemists, covering both theory and applications. The focus is set on existing as well as emerging methods for researchers, engineers, and practitioners active in the many and often interdisciplinary fields, where electrochemistry plays a key role. These fields will range – among others – from analytical and environmental sciences to sensors, materials sciences and biochemical research.

More information about this series at http://www.springer.com/series/7386

Oscar Alejandro Oviedo • Luis Reinaudi •
Silvana Graciela García •
Ezequiel Pedro Marcos Leiva

Underpotential Deposition

From Fundamentals and Theory to Applications at the Nanoscale

Springer

Oscar Alejandro Oviedo
Departamento de Matemática y Física
Facultad de Ciencias Químicas, INFIQC
Universidad Nacional de Córdoba
Córdoba, Argentina

Luis Reinaudi
Departamento de Matemática y Física
Facultad de Ciencias Químicas, INFIQC
Universidad Nacional de Córdoba
Córdoba, Argentina

Silvana Graciela García
Departamento de Ingeniería Química
Universidad Nacional del Sur
Bahía Blanca, Argentina

Ezequiel Pedro Marcos Leiva
Departamento de Matemática y Física
Facultad de Ciencias Químicas, INFIQC
Universidad Nacional de Córdoba
Córdoba, Argentina

ISSN 1865-1836 ISSN 1865-1844 (electronic)
Monographs in Electrochemistry
ISBN 978-3-319-24392-4 ISBN 978-3-319-24394-8 (eBook)
DOI 10.1007/978-3-319-24394-8

Library of Congress Control Number: 2015957586

Springer Cham Heidelberg New York Dordrecht London

Printed on acid-free paper

Springer International Publishing AG Switzerland is part of Springer Science+Business Media (www.springer.com)

Preface of Editor

There is no need to stress the importance of underpotential deposition (upd) for electrochemistry, surface science, and physics, both with respect to fundamental and applied studies, as upd belongs to the most widely studied and applied phenomena in electrochemical systems. Thus, it was very surprising that there did not exist a single monographic treatment of upd in the world literature. Overviews were only available in review papers, and special aspects of upd were covered in some books on metal deposition and electrocatalysis, to name but two. Rather short treatments of upd are available in textbooks, but a comprehensive description of the various experimental and theoretical aspects of upd and of its use for tuning electrochemical reactions was missing. I am very happy that four authors from Argentina, Ezequiel Pedro Marcos Leiva (Córdoba), Silvana Graciela García (Bahía Blanca), Oscar Alejandro Oviedo (Córdoba), and Luis Reinaudi (Córdoba), have accepted the request to write a monograph on underpotential deposition. The authors are internationally known for their contributions to the present state of understanding upd, and I am sure that this monograph will acquire the state of a classic book which every researcher will study and refer to when entering electrochemical deposition, electrocatalysis, or fundamental and applied surface science.

Greifswald, Germany — Fritz Scholz
July 2015

Techniques and Abbreviations

AES	Auger Electron Spectroscopy
AFM	Atomic Force Microscopy
DFT	Density Functional Theory
DRS	Differential Reflectance Spectroscopy
ECALE	Electrochemical Atomic Layer Epitaxy
EDL	Electrical Double Layer
EQCM	Electrochemical Quartz Crystal Microbalance
EXAFS	Extended X-Ray Absorption Fine Structure
FTIRS	Fourier Transform Infrared Spectroscopy
GDOES	Glow Discharge Optical Emission Spectroscopy
GIXS	Grazing Incidence X-Ray Scattering
IHP	Inner Helmholtz Plane
IRS	Infrared Spectroscopy
LEED	Low Energy Electron Diffraction
M	Metal
M_{ads}	Metal Adatom
MC	Monte Carlo
MD	Molecular Dynamics
ML	Monolayer
NPs	Nanoparticles
opd	Overpotential Deposition
PAS	Photoacoustic Spectroscopy
PDEIS	Potentiodynamic Electrochemical Impedance Spectroscopy
PZC	Potential of Zero Charge
RHEED	Reflection High Energy Electron Diffraction
RRDE	Rotating Ring-Disk Electrode
S	Substrate
SDD	Surface Differential X-Ray Diffraction
SHG	Second Harmonic Generation
S/M	Substrate and Adsorbate system
S@M	Substrate and Adsorbate Core-Shell Nanoparticle System

SCE	Saturated Calomel Electrode
SEM	Scanning Electron Microscopy
SERS	Surface Enhanced Raman Spectroscopy
SHE	Standard Hydrogen Electrode
SLRR	Surface-Limited Redox Replacement
SPM	Scanning Probe Microscopy
SRS	Specular Reflection Spectroscopy
STM	Scanning Tunneling Microscopy
SSE	Saturated Sulphate Electrode
SXS	Surface X-Ray Scattering
TPD	Temperature Programmed Desorption
TPS	Thermal Desorption Spectroscopy
TTL	Twin-Electrode Thin-Layer
UHV	Ultra High Vacuum
upd	Underpotential Deposition
XPS	X-Ray Photoelectron Spectroscopy

Contents

Chapter 1
Introduction

1.1 Underpotential Deposition: A Successful Misnomer?

The deposition of small amounts of metal atoms[1] on a foreign surface at potentials more positive that those predicted by Nernst equation is nowadays popularly known as underpotential deposition (upd). To denote something that involves positive quantities with the prefix under obviously appears as counterintuitive, so we devote a few lines to explain this contradictory denomination. In the fundamental field of the electrocrystallization of bulk metals, it is widely used the concept of overvoltage η, which is defined as:

$$\eta = E - E_{\mathrm{M_{(bulk)}/M^{z+}_{(aq)}}} \tag{1.1}$$

where E is the actual electrode potential, and $E_{\mathrm{M_{(bulk)}/M^{z+}_{(aq)}}}$ is the Nernst equilibrium potential of the reaction:

$$\mathrm{M_{(bulk)}} \rightleftarrows \mathrm{M^{z+}_{(aq)}} + z\mathrm{e}^- \tag{1.2}$$

where $\mathrm{M_{(bulk)}}$ represents the bulk metallic material, and $\mathrm{M^{z+}_{(aq)}}$ stands for an ion in solution, bearing the charge number z. Due to different kinetic hindrances, it always happens in the case of bulk materials that metal deposits take place when $E < E_{\mathrm{M_{(bulk)}/M^{z+}_{(aq)}}}$ so that in general the overvoltage results with the condition $\eta < 0$. Thus, in the case of bulk deposits the overvoltage results always in *negative* values of η. In the case of underpotential deposition, the reverse condition occurs, because

[1] By small amounts, we mean a number of atoms that is related to the number of atoms constituting the surface of a metal substrate. Thus, underpotential deposits usually involve submonolayers, monolayers or at the most bilayers.

O.A. Oviedo et al., *Underpotential Deposition*, Monographs in Electrochemistry,
DOI 10.1007/978-3-319-24394-8_1

metal deposition takes place for $E > E_{M_{(bulk)}/M^{z+}_{(aq)}}$, so that $\eta > 0$. Then, since the term *over*voltage was already reserved for metal deposition in the $\eta < 0$ condition, the only possibility left was to denominate the situation $\eta > 0$ as *under*voltage, from there the term *under*potential deposition, which is usually shortened as upd.

1.2 The Magic World of Metal Underpotential Deposition

Within electrochemical surface processes, the deposition of a metal onto a foreign metal surface at underpotential opens the way to a whole universe of possibilities for preparing and designing surfaces with a variety of applications. Among them, we can mention electrocatalysis [1–5], production of compound semiconductors [6, 7], determination of metal traces by stripping voltammetry, achieving mercury-free electroanalytical procedures [8–10], design of biosensors [11–14], surface area measurement of metals [15, 16], of particular importance for metallic nanoporous materials [17, 18], design of nanoparticle shape [19–21] and composition [22, 23], fabrication of nanocables [24], nanotripods [25], microstructures with improved Surface Enhanced Raman Spectroscopy activity [26], evaluation of overpotential deposition kinetics of reactive metals [27], etc. The previous enumeration is by no means mutually exclusive, since for example nanoparticle synthesis is oriented to catalysis, and we emphasize that it is just mentioned some sample reviews or recent work.

Since upd involves the growth of a new phase in a two dimensional system, we will see along the chapters of this book that this phenomenon is by itself of fundamental importance for understanding a number of related processes involved in the formation of new phases with this dimensionality.

We illustrate with the aid of Fig. 1.1 the key advantage of electrochemical deposition of a metal concerning adsorption studies, with respect to the same processes achieved from the gas phase. Let us represent the desorption of an adatom M from a substrate S according to the reaction:

$$S - M \rightleftarrows S + M_{vac} \tag{1.3}$$

where M_{vac} represents a metal atom in vacuum. In Fig. 1.1 we show schematically the (free) energy of an atom bonded to a surface as a function of the distance from it. In the case of metallic substrate/adsorbate systems, the binding energy curve exhibits typically a minimum with values in the range $-3 \leq E_{ads}(\text{eV}) \leq -5$ with respect to the vacuum level [28], indicating that the desorption energy E_{des} must be of this order of magnitude (but with opposite sign). If we consider the thermal energy at room temperature, $k_B T = 0.025$ eV, we see that the E_{des} amounts are

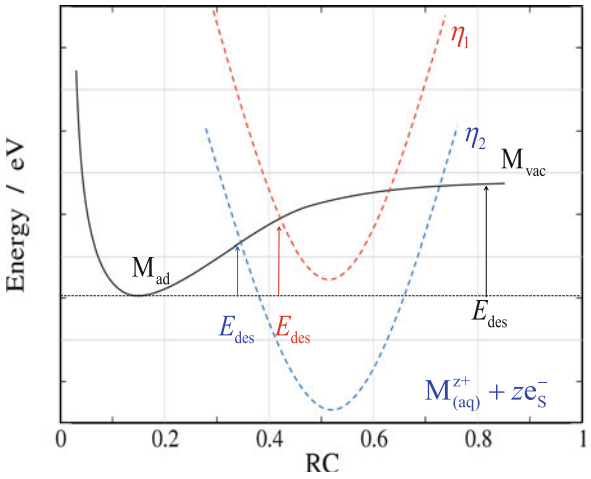

Fig. 1.1 Schematic comparison between the desorption of a metal adatom from a metal surface by physical detachment (*continuous line*) and electrochemical oxidation (*broken lines*). The *full line* illustrates the free energy curve of the adatom as function of the distance from the surface (*RC* reaction coordinate). The *dotted lines* represent the potential energy of the cations in solution plus the electron located in the metal for two different overpotentials, where $\eta_2 < \eta_1$. The *arrows* show the point where the potential energy of the adatom and the ion plus electron systems meet. The heights of these arrows give an idea of the activation energy for the detachment process (E_{des})

between 120 and 200 k_BT. Taking into account these figures we can make an estimation of the thermal desorption time of an adatom according to:

$$\frac{1}{t_{des}} = \nu \ \exp[-E_{des}/k_BT] \tag{1.4}$$

where the preexponential factor ν contains entropic contributions and shows a weak dependence on the temperature and E_{des} has been taken as a measure for the activation energy of the desorption process. Inserting into Eq. (1.4) the mentioned limits for E_{des}, and approximating $\nu \approx 1 \times 10^{13}\ s^{-1}$, we get that the desorption times should be in the range $1 \times 10^{40} < t_{des}(s) < 7 \times 10^{73}$. This means that even if we monitor a macroscopic ensemble of adsorbed particles, let us say, of the order of $\sim 10^{23}$, we would find desorption times in the interval $1 \times 10^{17} < t^{macro}_{des}(s) < 7 \times 10^{50}$. To bring into scale the previous curves, we remind that the estimated age of the universe is $t_{univ} \approx 4 \times 10^{18}$ s. Thus, we arrive to the conclusion that the achievement at room temperature of adsorption/desorption equilibrium is not possible for most S/M metal couples, due to the fact that one of the processes (desorption) is kinetically impossible to achieve. Of course, the previous profiles may be drastically altered by increasing the temperature, but doing this would also promote other processes, like alloying, which are not wished if one is interested on

adsorption studies. What electrochemistry does, as illustrated in the red and the blue lines of Fig. 1.1 is to change reaction (1.3) into:

$$S - M \rightleftarrows S + M^{+z}_{(aq)} + ze^{-} \tag{1.5}$$

The dotted curves in Fig. 1.1 introduces an alternative state to that of the desorbed adatom, where now the final state is an ion in solution $M^{+z}_{(aq)}$ and an electron (or the number of electrons corresponding to the valence) in the substrate electrode. Since the latter may be polarized, the free energy of electrons in the metal may be changed accordingly, and the desorption barrier may be lowered, as it is indicated by the red and blue arrows in the Fig. 1.1 for two different surface polarizations. It can be seen that the decrease of the barrier for adatom desorption, concomitantly increases the barrier for adsorption. Of course, reality is far more complex than this simple picture and a full theory able to calculate the adsorption and desorption rates accurately for metallic systems is still not available, but the figure illustrates the main idea beyond the electrochemical manipulation of substrate/adsorbate metallic systems, in comparison with a similar process in the gas phase.

From Fig. 1.1 we also visualize that in electrochemistry, the exchange rate between ions in solution and adatoms will be governed by the height of the energy barrier to be surmounted between adatoms and ions, so that it will be determined by the properties of both the metal surface and the solution. This problem has been the subject of extensive consideration in electrochemical textbooks [29] and its nature is starting to be elucidated for specific systems in very recent theoretical work [30].

As stated above, the occurrence of the upd phenomenon results in the formation of a two- dimensional phase, involving in some cases nucleation and growth processes, which take place under the influence of a potential difference [29]. Although the situation is in several aspects similar to the growth of a bulk metallic (three dimensional) phase under electrochemical conditions, there are important differences to take into account.

To go more properly into the peculiarities of upd, let us consider first the problem of the deposition of a bulk metal under equilibrium conditions. This can be described, as it is well known, by a Nernst diagram as the one depicted in Fig. 1.2a. The diagram shows the equilibrium potential $E_{M_{(bulk)}/M^{z+}_{(aq)}}$ for reaction (1.2) as a function of the logarithm of the activity of the cation $a_{M^{z+}_{(aq)}}$, which is given by:

$$E_{M_{(bulk)}/M^{z+}_{(aq)}} = E^{0}_{M_{(bulk)}/M^{z+}_{(aq)}} + \frac{RT}{zF}\ln\left(\frac{a_{M^{z+}_{(aq)}}}{a_{M_{(bulk)}}}\right) \tag{1.6}$$

where $E^{0}_{M_{(bulk)}/M^{z+}_{(aq)}}$ is the standard equilibrium potential, $a_{M_{(bulk)}}$ is the activity of the bulk solid (generally assumed to be equal to 1), T is the temperature, R and F correspond to the gas and Faraday constants, respectively. This Figure can be

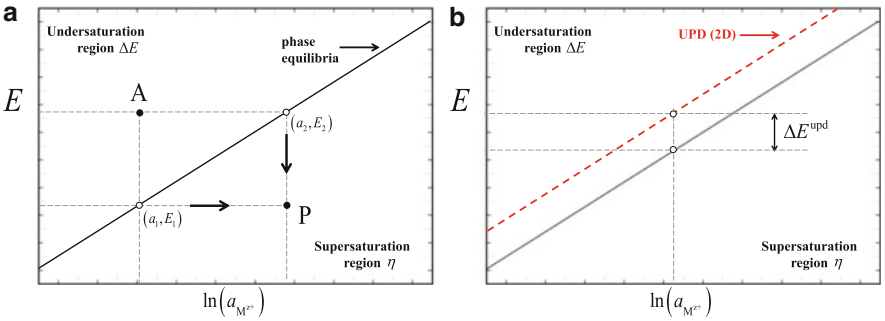

Fig. 1.2 Qualitative scheme of the variation of the equilibrium dissolution/deposition potential of a metal as a function of ion activity. (**a**) Case of dissolution/deposition of a bulk metal, see Eq. (1.2) in the text. (**b**) Case of underpotential dissolution/deposition of metal M on a foreign substrate S, see Eq. (1.5) in the text. The *continuous black curve* shows the equilibrium conditions for piece of a bulk metal, the *broken red curve* shows the equilibrium line for underpotential deposition conditions. The distance between the two curves is the underpotential shift, ΔE^{upd}

envisaged as a phase diagram, where the line denotes coexistence points of the solid phase with the ions in solution and the electrons in the metal. Points above and below the line correspond to situations where, if we force the system to be there, a non-equilibrium state will be reached. For example, if we bring the system to point A, characterized by the pair $(a_1^{\text{A}}, E_2^{\text{A}})$, spontaneous metal dissolution will take place. Alternatively, bringing the system to the conditions of point P, characterized by the pair $(a_2^{\text{P}}, E_1^{\text{P}})$, will result in spontaneous metal deposition. For this reason, we have denoted the previous regions as undersaturation and oversaturation regions respectively.

There are several ways to take the system into these non-equilibrium regions. Let us consider for example the two ways considered in the arrows marked in the Fig. 1.2a, to bring the system to point P, from two different initial equilibrium situations:

1. Increasing $a_{\text{M}^{z+}_{(\text{aq})}}$ at a constant E (horizontal arrow).
2. Decreasing E, at a constant $a_{\text{M}^{z+}_{(\text{aq})}}$ (vertical arrow).

These processes are marked in Fig. 1.2a as processes $(a_1, E_1) \rightarrow \text{P}$ and $(a_2, E_2) \rightarrow \text{P}$. Both take to the same point on the oversaturation region, leading to nucleation and growth of the bulk solid phase $\text{M}_{(\text{bulk})}$. It is interesting to note the dual way that electrochemistry provides to induce nucleation and growth of a new phase. The first path described above has been employed to induce localized electrodeposition using a STM tip [31]. Path 2 is the usual way employed to induce metal growth by a potentiostatic pulse [31, 32].

As mentioned in Eq. (1.1), the magnitude quantifying this displacement from equilibrium is the overpotential η, in such a way that $\eta < 0$ indicates oversaturation (cathodic overpotentials) and $\eta > 0$ indicates undersaturation (anodic overpotentials), while $\eta = 0$ corresponds to phase coexistence.

Although we will see that the proper thermodynamic treatment of upd involves a number of complex features, intuitive knowledge can be gained by proposing in the case of underpotential deposits an heuristic (and rough) extension of Nernst Eq. (1.6) by writing:

$$E_{(\mathrm{M}_\theta/\mathrm{S})/\mathrm{M}^{z+}_{(\mathrm{aq})}} = E^0_{\mathrm{M}_{(\mathrm{bulk})}/\mathrm{M}^{z+}_{(\mathrm{aq})}} + \frac{RT}{zF}\ln\left(\frac{a_{\mathrm{M}^{z+}_{(\mathrm{aq})}}}{a_{\mathrm{M}_\theta/\mathrm{S}}}\right) \tag{1.7}$$

where $E_{(\mathrm{M}_\theta/\mathrm{S})/\mathrm{M}^{z+}_{(\mathrm{aq})}}$ denotes the potential at which the $\mathrm{M}^{z+}_{(\mathrm{aq})}$ ions are in equilibrium with the M atoms adsorbed on the surface of S at the coverage θ. $a_{\mathrm{M}_\theta/\mathrm{S}}$ is the activity of M adsorbed on S at the coverage θ. In the limit of multilayer adsorption, Eq. (1.7) reduces to Eq. (1.6), that is, $a_{\mathrm{M}_\theta/\mathrm{S}} \to a_{\mathrm{M}_{(\mathrm{bulk})}} = 1$ and $E_{(\mathrm{M}_\theta/\mathrm{S})/\mathrm{M}^{z+}_{(\mathrm{aq})}} \to E_{\mathrm{M}_{(\mathrm{bulk})}/\mathrm{M}^{z+}_{(\mathrm{aq})}}$.

In the case of a bulk or surface alloy, $a_{\mathrm{M}_\theta/\mathrm{S}}$ decreases with the decreasing fraction of M in the alloy [2, 33]. In the case of monolayers or submonolayers, $a_{\mathrm{M}_\theta/\mathrm{S}}$ turns into a function of the surface coverage by adatoms. The presence of a monolayer occurring at underpotentials is equivalent to consider $a_{\mathrm{M}_\theta/\mathrm{S}} < 1$, so that all equilibrium potentials are shifted upwards, $E_{(\mathrm{M}_\theta/\mathrm{S})/\mathrm{M}^{z+}_{(\mathrm{aq})}} > E_{\mathrm{M}_{(\mathrm{bulk})}/\mathrm{M}^{z+}_{(\mathrm{aq})}}$, see Fig. 1.2b. As a consequence of this shift, the upd curve (red line) falls in the undersaturation region with respect to the bulk equilibrium (black line). That is, the metal M exists on the surface of S at potentials where it should not occur if we think in terms of the bulk M material!.

In the case of upd, a magnitude that may be quantified is the so-called underpotential shift, denoted with ΔE^{upd} in Fig. 1.2b. Using Eqs. (1.6) and (1.7) we see that ΔE^{upd} is given by:

$$\Delta E^{\mathrm{upd}} = E_{(\mathrm{M}_\theta/\mathrm{S})/\mathrm{M}^{z+}_{(\mathrm{aq})}} - E_{\mathrm{M}_{(\mathrm{bulk})}/\mathrm{M}^{z+}_{(\mathrm{aq})}} \tag{1.8}$$

so that $\Delta E^{\mathrm{upd}} > 0$ indicates the presence of phases more stable than the prediction of Nernst equation.

As we will see in Chap. 3, the previous argumentation falls too short of being an accurate description, and the curves in Fig. 1.2b do not run parallel. However, we have gained an intuitive introduction to the concept of underpotential shift.

A further complication arises due to the fact that the surface of a real metal electrode is not a perfect arrangement of adsorption sites, but contains a number of imperfections like steps (one-dimensional), kinks and vacancies (zero-dimensional). These defects provide adsorption sites for the formation of deposits that are energetically more favorable than the formation of the monolayer. Thus, if we think in terms of a surface that is progressively polarized towards increasingly negative overpotentials, monolayer growth is preceded by the formation of structures of lower dimensionality [34]. Figure 1.3 shows schematically some of these structures.

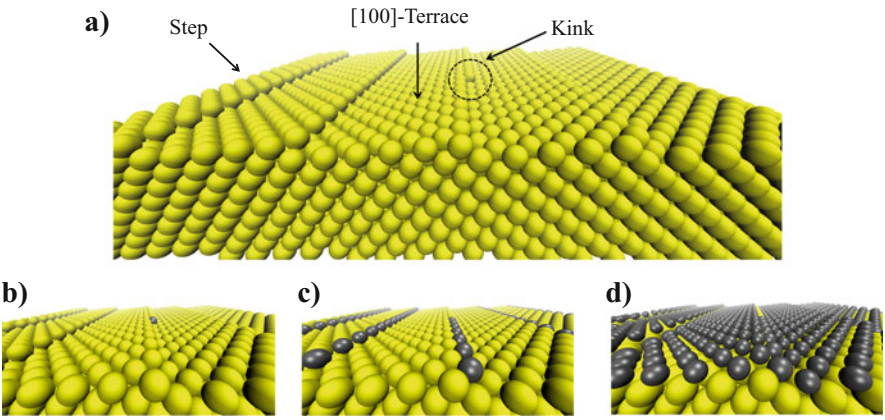

Fig. 1.3 Stepwise formation of structures of low dimensionality upon application of decreasing overpotentials: (**a**) defective surface, (**b**) kink decoration, (**c**) step decoration, and (**d**) monolayer formation

To account for the formation of metallic phases with different dimensionalities, an effective Nernst equation may be also proposed:

$$E_{(\mathrm{M_{iD}/S})/\mathrm{M}^{z+}_{(aq)}} = E^{0}_{\mathrm{M_{(bulk)}}/\mathrm{M}^{z+}_{(aq)}} + \frac{RT}{zF}\ln\left(\frac{a_{\mathrm{M}^{z+}_{(aq)}}}{a_{\mathrm{iD}}}\right) \qquad \text{with i} = 0,\ 1 \text{ and } 2 \tag{1.9}$$

where $E_{(\mathrm{M_{iD}/S})/\mathrm{M}^{z+}_{(aq)}}$ is the potential at which the $\mathrm{M}^{z+}_{(aq)}$ ions are in equilibrium with M atom adsorbed on the iD-structure of S, $E^{0}_{\mathrm{M_{(bulk)}}/\mathrm{M}^{z+}_{(aq)}}$ is the corresponding standard potential and a_{iD} is an activity, function of structure and dimensionality. The concept of underpotential shift may also be extended according to:

$$\Delta E^{\mathrm{upd}}(\mathrm{iD}) = E_{(\mathrm{M_{iD}/S})/\mathrm{M}^{z+}_{(aq)}} - E_{\mathrm{M_{(bulk)}}/\mathrm{M}^{z+}_{(aq)}} \qquad \text{with i} = 0,\ 1 \text{ and } 2 \tag{1.10}$$

Figure 1.4 shows in blue the equilibrium curves corresponding to these low dimensional structures, which follow the ordering:

$$E_{(\mathrm{M_{0D}/S})/\mathrm{M}^{z+}_{(aq)}} > E_{(\mathrm{M_{1D}/S})/\mathrm{M}^{z+}_{(aq)}} > E_{(\mathrm{M_{2D}/S})/\mathrm{M}^{z+}_{(aq)}} > E_{\mathrm{M_{(bulk)}}/\mathrm{M}^{z+}_{(aq)}} \tag{1.11}$$

where the upd shifts are expected to follow the ordering:

$$\Delta E^{\mathrm{upd}}(0\mathrm{D}) > \Delta E^{\mathrm{upd}}(1\mathrm{D}) > \Delta E^{\mathrm{upd}}(2\mathrm{D}) \tag{1.12}$$

Depending on the magnitude of these differences, several current peaks or their convolution may be present.

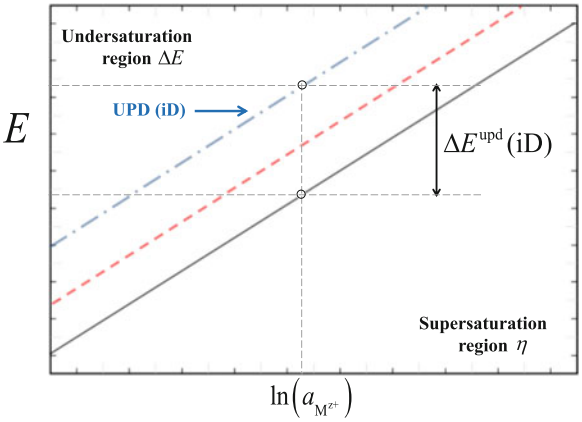

Fig. 1.4 Qualitative scheme for the variation of the equilibrium dissolution/deposition potential as a function of cation activity. The *continuous black curve* corresponds to equilibrium conditions for a bulk metal surface, the *broken red curve* shows the equilibrium line for 2D underpotential dissolution/deposition and the *blue dotted-broken line* shows the equilibrium condition for underpotential dissolution/deposition of i-Dimensional structures, with i <2

The largest contribution to ΔE^{upd} is given by the magnitude of the M − S binding energy, determined by the following factors [33]:

(i) the lateral and vertical binding energies between metallic adatoms in nanostructures and the binding energy between adatoms and the substrate,
(ii) the energetic influence of local surface defects of the substrate,
(iii) the binding energies between solvent dipoles and the metallic substrate/ nanostructure system, and
(iv) the binding energies of solvated anions with S and the metallic nanostructure.

While the first two factors are relatively straightforward to evaluate in terms of models taking into account the metal nature of adsorbate and substrate, the third and fourth elements involve very different interactions (i.e. van der Waals, ionic), which require approximations of considerable complexity.

Concerning effects at the nanoscale, Plieth [35] showed that the equilibrium potential of nanoparticles (NPs), $E_{\mathrm{M_{(NP)}}/\mathrm{M^{z+}_{(aq)}}}$, of a given metal shifts towards more negative potentials with decreasing size. This corresponds to an increase in the free energy of the system and the effect is consistent with an increase in the activity of the metal, that is, $a_{\mathrm{M_{(NP)}}} > 1$. This behaviour is a consequence of the increasing surface energy of the NP and/or its increasing curvature. The green curve in Fig. 1.5 shows the hypothetical $E_{\mathrm{M_{(NP)}}/\mathrm{M^{z+}_{(aq)}}}$ vs $\ln(a_{\mathrm{M^{z+}}})$ curve, exhibiting a negative potential shift, where it is shown that the stability of the pure metal M-NP occurs in the supersaturation region. In other words, a nanoparticle of a pure metal M dissolves at potentials where this bulk metal subsists in equilibrium.

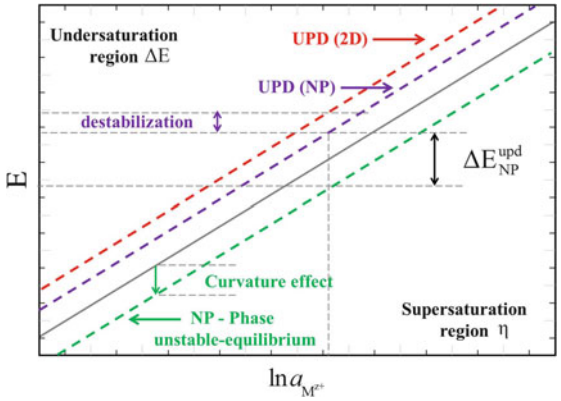

Fig. 1.5 Qualitative scheme of the variation of the deposition potential as a function of the ion activity for underpotential deposition at the nanoscale. The *continuous black curve* corresponds to equilibrium conditions for a piece of a bulk metal, the *broken red curve* shows the equilibrium line for 2D underpotential deposition, the *green broken line* shows the condition of unstable equilibrium for a metal nanoparticle and the *magenta broken line* show the underpotential deposition on a nanoparticle

However, an underpotential deposit of M on a NP made of a different metal S could in principle show the behaviour depicted by the curve in magenta in Fig. 1.5: it should be less stable than the 2D deposit of M on S (curve in red), but may be more stable than the bulk metal M (curve in black). Thus, the occurrence of upd on NPs will be the result of a delicate balance between substrate/adsorbate interaction and curvature effects, which will be in turn determined by NP size. Chapter 6 is fully dedicated to this type of problems.

1.3 Pre-history and Rise of upd

Starting from a very wide viewpoint, we can state that electrochemistry is nowadays a mature science, whose origins dates back to the work of Galvani and Volta, at the end of eighteenth and the beginning of the nineteenth centuries. Its aim is the study of the structure of the interphase between an electric conductor (denominated electrode) and an ionic conductor (denominated electrolyte), or the interphase between two electrolytes [36], and the processes that take place at these interphases. The interphase is the transition region between both phases; its properties differ significantly from those of the corresponding bulk phases. In contrast to this well established knowledge, the recognition of the fact that small quantities of metals may be deposited at potentials more positive than the Nernst reversible potential is relatively more recent. At the beginning, this phenomenon drew particular attention from electrochemists, since at that time the process of nucleation and growth of a

new phase was thought to be a rather simple phenomenon, and not a process involving different stages, as known nowadays.

The first indications for the upd phenomenon were given by Haissinsky in his research on the deposition of radioactive materials [37]. This author [38–40] argued that this phenomenon was due to lattice sites of the substrate presenting large adsorption energies (so called "active centers"). Far from the upd current denomination, at that time the process was addressed as deposition of small metal traces from extremely diluted solutions [41–43]. Shortly after this work, other authors started research on this topic, as for example Rogers [44–52], Kolthoff [53], Haenny [54, 55] and Bowles [56–61]. Current-potential curves (voltammograms) started to be used to analyze traces of Ag deposited on Pt, Cd, Zn and small amounts of Pb on mercury-plated platinum [62–64]. It was soon established that the deposition of these metal traces was very sensitive to the substrate material, and the first attempt to interpret upd through a thermodynamic model was undertaken by Rogers in 1949 [65, 66]. Up to that moment, there was a great controversy concerning the applicability of Nernst equation to describe the deposition potential of these metal traces. The work of Rogers [65] showed the need to consider all the terms in Nernst equation, including the activity of the solid, to describe this phenomenon. Based on the concept drawn by Herzfeld [67] that the activity $a_{M_\theta/S}$ of a metal adsorbed on a surface varies proportionally with the fraction of surface covered, θ:

$$a_{M_\theta/S} = f_2\theta \tag{1.13}$$

where the proportionality constant, f_2, is denominated activity coefficient of the metal deposit, Rogers [65] proposed a modification to Nernst equation:

$$E = E^0 - E_a - \frac{RT}{zF}\ln\left(\frac{A_e f_1}{VN_a A_a f_2}\left(\frac{C_{ox}}{C - C_{ox}}\right)\right) - \frac{bRT}{zF}\ln\left(C_g f_g\right) \tag{1.14}$$

where f_1 is the activity coefficient of the ion, C_{ox} is the equilibrium concentration of reducible ion, C is initial molar concentration of reducible (or oxidizable) ions, N_a is Avogadro's number, A_a and A_e are cross-sectional area, in cm^2, of an atom of deposit and area of the electrode in cm^2, respectively. The last term in Eq. (1.14) is introduced to consider the activity of a possible complex formed by the ion. The index g denotes the complex molecule, having b ligands coordinated with the metal ion being deposited. To consider the changes in the free energy of adsorption, Rogers introduced a new term, E_a in Eq. (1.14), accounting for the difference between the deposition potential of the metal ion on a surface of similar nature and the deposition potential on a foreign one. Thus, if $E_a > 0$, the deposit should be more noble than predicted by Nernst equation. Shortly after the previous contribution, the first indication was found by Mills et al. in 1953 [68] for the dependence of the deposition potential of a given adsorbate on the chemical nature of the substrate electrode. These authors showed that Pb deposition on Au starts at 0.2 V more positive potentials than the deposition potential found on Ag surfaces.

In 1956 Nicholson [69] presented the first computational application to upd, solving numerically [70, 71] the electrochemical problem along with second Fick's law in an IBM 650 computer. This author found a good agreement between the model and experimental data for Ag and Pb deposition on Pt, but found important deviations for Cu deposition on Pt.

Concerning the relationship of upd with early ultra-high vacuum (UHV) experiments on related systems, the articles of Newman [72, 73] and Gruenbaum [74] in UHV showed the presence of a Pb monolayer (and fractions of it) on a Au(111) surface, and evidenced a layer by layer growth up to four monolayers, but the extrapolation to electrochemical systems was not straightforward.

In the 1960s, some authors started to denominate upd as "undervoltage effect" [75], and this phenomenon started to become of wider interest and deserved intensive research [76]. Table 1.1 summarizes work in the area developed in the 1960s decade.

In 1974, Gerischer, Kolb and Przasnyski [94, 95] proposed the first phenomenological theory to explain the origin of upd. Their research on the upd phenomenon showed that the potential difference between upd and bulk deposition could be related to the work function difference between substrate and adsorbate. These authors suggested that the ionic contribution of the bond between the adsorbate and the substrate, given by the partial electron transfer, is the main driving force of the phenomenon. This assumption was supported by the subsequent work of Vijh [96]. Other contributions, like the surface structure of the substrate, the effect of anions

Table 1.1 Compilation of experimental work undertaken in the 60s concerning upd

Substrate	Adsorbate	References
Pt	Ag	[77]
	Pb	[77, 78]
	Cu	[61, 77, 79–83]
	Ni	[84]
	Au	[84]
	Ce	[78, 85, 86]
	Tl	[56, 57, 61, 86]
	Bi	[61, 78]
	Cd	[61]
	Sn	[61, 60]
Graphite	Hg	[87]
	Ag	[88]
	Cu	[81, 89]
Au	Ni	[84]
	Ag	[75]
	Pb	[90, 91]
Ag	Pb	[76, 92]
	Tl	[76, 93]
Pb	Cd	[76]

and the occurrence of submonolayers or bilayers were not included in this modeling.

At the beginning of the 1970s, attention of experimentalists was focused on the charge status of adsorbates and the effect of the nature of the substrate. Schulze et al. [97–99] and Lorenz et al. [100] reviewed the state-of-the-art of the concept of electrosorption valency at that time. While this concept will be developed in detail in Chap. 3, we advance that it is related to the flow of charge during the electrosorption process. At difference with the Nerstian or Faradaic valence, the electrosorption valency is generally a non-integer number. At the middle of the 1970s different authors showed the importance of performing experiments with well defined metal surfaces, the era of upd on single crystal surfaces was beginning [101–120]. The joint use of electrochemical techniques with Low Energy Electron Diffraction (LEED), Reflected High Energy Electron Diffraction (RHEED), Auger Electron Spectroscopy (AES), Ellipsometry and in situ Specular Reflection Spectroscopy (in situ-SRS) allowed to analyze surface reconstructions, deformations, thicknesses [105, 110, 111, 114, 121–123], different growth types [105, 115], expanded structures like on (100) and (111) surfaces [107, 114], including the occurrence of a second upd monolayer [103].

The study of upd on single crystal surfaces also shed light on nucleation and growth of two-dimensional structures [101, 116, 124–126]. The voltammograms showed better defined and sharper peaks than those obtained with polycrystalline surfaces, and the current-time potentiostatic transients showed possible evidence for the occurrence of first-order phase transitions, or at least the existence of attractive interactions. The possibility of studying these phenomena started to spread over the different research groups. However, the definite answer to some of the questions that arose from these studies is still pending, as we will see along Chaps. 3 and 5. The multiple peaks found in the voltammograms obtained with single crystals rapidly turned into an active subject of research [66–68, 75, 77–93, 126].

The wide research with single crystal surfaces along the 1970s showed that the correlations found by Gerischer, Kolb and Przasnyski [94, 95] could only be applied semiquantitatively to polycrystalline surfaces, since the actual situation concerning single crystal surfaces is considerably more complex [107, 127]. The concept of a binding energy only determined by electronegativity effects was found as insufficient, and the need for more complex models taking into account surface geometry and lateral interactions emerged.

1.4 Upd Under the Loupe: Then and Now

In the 1980s the study of upd was favored by the great synergy between the high degree of surface control offered by single crystals and the development of new and powerful surface techniques. The possibility of direct imaging of surfaces and the availability of structural information in direct and reciprocal space gave many answers in the upd field and opened many other ones. Chapters 2 and 3 deal with

these and other studies. The great flexibility of upd to generate surfaces with mixed properties motivated a great body of work using upd systems as model catalytic systems. Chapter 4 deals with application of upd to electrocatalysis.

The massification on computer use, the increasing computer power appearing in the 1990s, as well as the development of new software allowed performing virtual experiments (simulations) of increasing complexity for upd. Chapter 5 reports on these advances.

The advent of nanoscience in the 1990s also reached upd applications in this field, though with a decade of delay. Chapter 6 describes this emerging research area, where upd and galvanic replacement appear as a powerful tool for the design of new materials in the nanoscale.

The new trends and perspectives for upd will be described in Chap. 7.

References

1. Kokkinidis G (1986) J Electroanal Chem 201:217
2. Parsons R, VanderNoot T (1988) J Electroanal Chem 257:9
3. Jarvi TD, Stuve EM (1998) In: Lipkowski J, Ross A (eds) Electrocatalysis. Wiley-VCH, New York
4. Sánchez CG, Leiva EPM (2003) Handbook of fuel cell technology. In: Vielstich W, Lamm A, Gasteiger H (eds) Chapter 5, Catalysis by upd metals, vol 2. Wiley, Chichester, pp 47–61
5. Adzic RR (2007) Electrocatalysis on surfaces modified by metal monolayers deposited at underpotentials. In: Encyclopedia of electrochemistry. Wiley-VCH, Weinheim
6. Gregory BW, Stickney JL (1991) J Electroanal Chem 300:543
7. Wade TL, Vaidyanathan R, Happek U, Stickney JL (2001) J Electroanal Chem 500:322
8. Beni V, Newton HV, Arrigan DWM, Hill M, Lane WA, Mathewson A (2004) Anal Chim Acta 502:195
9. Herzog G, Arrigan DWM (2005) Trends Anal Chem 24:208
10. Herzog G, Beni V (2013) Anal Chim Acta 769:10
11. Aluoch AO, Sadik OA, Bedi G (2005) Anal Biochem 340:136
12. Noah NM, Marcells O, Almalleti A, Lim J, Sadik OA (2011) Electroanalysis 23:2392
13. Li Y, Lu Q, Wu S, Wang L, Shi X (2013) Biosens Bioelectron 41:576
14. Oua K-L, Hsue T-C, Liud Y-C, Yang K-H, Tsai H-Y (2014) Anal Chim Acta 806:188
15. Chen D, Tao Q, Liao LW, Liu SX, Chen YX, Ye S (2011) Electrocatal 2:207
16. Shao M, Odell JH, Choi S-I, Xia Y (2013) Electrochem Commun 31:46
17. Liu Y, Bliznakov S, Dimitrov N (2009) J Phys Chem C 113:12362
18. Rouya E, Cattarin S, Reed ML, Kelly RG, Zangari G (2012) J Electrochem Soc 159:K97
19. Langille MR, Personick ML, Zhang J, Mirkin CA (2012) J Am Chem Soc 134:14542
20. Personick ML, Mirkin CA (2013) J Am Chem Soc 135:18238
21. Yu Y, Zhang Q, Xie J, Lee JY (2013) Nat Commun 4:1454
22. Jiang Y, Jia Y, Zhang J, Zhang L, Huang H, Xie Z, Zheng L (2013) Chem Eur J 19:3119
23. Wu Q, Li Y, Xian H, Xu C, Wang L, Chen Z (2013) Nanotechnology 24:025501
24. Jie-Ren K et al (2006) U. S. pattern no. 20060024438 A1, Feb 2, 2006
25. Zhang L, Choi S-I, Tao J, Peng H-C, Xie S, Zhu Y, Xie Z, Xia Y (2014) Adv Funct Mater 24:7520
26. Plowman BJ, Abdelhamid ME, Ippolito SJ, Bansal V, Bhargava SK, O'Mullane AP (2014) J Solid State Electrochem 18:3345

27. Guerra E, Kelsall GH, Bestetti M, Dreisinger D, Wong K, Mitchell KAR, Bizzotto D (2004) J Electrochem Soc 151:E1
28. See for example typical cohesive energies of metals in Kittel C (2005) Introduction to solid state physics, 8 edn. Wiley, New York
29. Budevski E, Staikov G, Lorenz WJ (1996) Electrochemical phase formation and growth. VCH, Weinheim
30. Pinto LMC, Spohr E, Quaino P, Santos E, Schmickler W (2013) Angew Chem 125:8037
31. Mariscal MM, Dassie SA (eds) (2007) Recent advances in nanoscience. Research Signpost, Trivandrum-Kerala
32. Lipkowski J, Ross PN (1999) Imaging of surfaces and interfaces. Wiley-Vch, New York
33. Oviedo OA, Mayer CE, Staikov G, Leiva EPM, Lorenz W (2006) J Surf Sci 600:4475
34. Staikov G, Lorenz WJ, Budevski E (1999) In: Ross P, Lipkowski J (eds) Imaging of surfaces and interfaces – frontiers of electrochemistry, vol 5. Wiley-VCH, New York, p 1
35. Plieth WJ (1982) J Phys Chem 86:3166
36. Schmickler W (1996) Interfacial electrochemistry. Oxford University Press, New York
37. Haissinsky M (1933) Chim Phys 30:27
38. Haissinsky M (1946) Electrochimie des Substances Radioactives et des solutions extêmement diluées. Actual, Scient No. 1009. Hermann, Paris
39. Haissinsky M (1946) J Chim Phys 43:21
40. Haissinsky M (1946) J Chim Phys 41:21
41. Haissinsky M, Coche A (1949) J Chem Soc:S397
42. Haissinsky M (1952) Ezperientia 8:12
43. Danon J, Haissinsky M (1951) Chim Phys 48:135
44. Rogers LB, Krause DP, Griess JC Jr, Ehrlinger DB (1949) J Electrochem Soc 95(2):33
45. Griess JC Jr, Byrne JT, Rogers LB (1951) J Electrochem Soc 98(11):447
46. Rogers IB, Stehney AF (1949) J Electrochem Soc 96:25
47. Rogers LB, Miller HH, Goodrich RB, Stehney AF (1949) Anal Chem 21:777
48. Byrne JT, Rogers LB (1951) J Electrochem Soc 98(11):457
49. Byene JT, Rogers LB, Griess JC Jr (1951) J Electrochem Soc 98(11):452
50. Rogers LB (1955) Rec Chem Prog 16:197
51. Rogers LB, Merritt C Jr (1953) J Electrochem Soc 100(3):131
52. De Geiso RC, Rogers LB (1959) J Electrochem Soc 106(5):433
53. Kolthoff IM, Tanaka N (1954) Anal Chem 26(4):632
54. Haenny C, Mivalez P (1948) Helv Chim Acta 31:633
55. Haenny C, Reymond P (1954) Helv Chim Acta 37:2067
56. Bowles BJ (1965) Electrochim Acta 10:717
57. Bowles BJ (1965) Electrochim Acta 10:731
58. Bowles BJ (1965) Electrochim Acta 15:589
59. Bowles BJ (1965) Electrochim Acta 15:737
60. Bowles BJ, Cranshaw TE (1965) Phys Lett 17:258
61. Bowles BJ (1966) Nature 212:1456
62. Lord SS Jr, O'Neill RC, Rogers LB (1952) Anal Chem 24:209
63. Gardiner KW, Rogers LB (1953) ibid 25:1393
64. Marple TL, Rogers LB (1954) Anal Chem Acta 11:574
65. Rogers LB, Stelmey AF (1949) J Electrochem Soc 95:25
66. Griess JC, Byrne JT, Rogers LB (1951) J Electrochem Soc 98:447
67. Herzfeld KF (1913) Phys Z 13:29
68. Mills T, Willis GH (1953) J Electrochem Soc 100:452
69. Nicholson MM (1957) J Am Chem Soc 79(1):7
70. Rutledge G (1932) Phys Rev 40:262
71. Wagner C (1954) J Math Phys 32:289
72. Newman RC (1955) Ph.D. Thesis, University of London
73. Newman RC (1957) Philos Mag 2:750
74. Gruenbaum E (1958) Proc Phys Soc Lond 72:459
75. Probst RC (1968) J Electroanal Chem 16:319

76. Astley DJ, Harrison JA, Thirsk HR (1968) J Electroanal Chem 19:325
77. Nisbet AR, Bard A (1963) J Electroanal Chem 6:332
78. Madi I (1961) J Inorg Nucl Chem 22:169
79. Kublik Z (1963) J Electroanal Chem 5:450
80. Breiter MW (1967) J Electrochem Soc 114:1125
81. Breiter MW (1969) J Electroanal Chem 23:173
82. Napp DT, Bruckenstein S (1958) Anal Chem 40:1036
83. Tindall GW, Bruckenstein S (1968) Anal Chem 40:1051
84. Nicholson MM (1960) Anal Chem 32:1058
85. Madi I (1954) J Inorg Nucl Chem 26:2149
86. Madi I (1962) J Inorg Nucl Chem 24:1501
87. Perone SP, Kretlow J (1965) Anal Chem 37:968
88. Perone SP (1963) Anal Chem 35:2091
89. Vassos BH, Mark HB Jr (1967) J Electroanal Chem 13:1
90. Schmidt E, Gygax HR (1967) J Electroanal Chem 13:378
91. Schmidt E, Gygax HR (1967) J Electroanal Chem 14:126
92. Schmidt E, Siegenthaler H (1969) Helv Chim Acta 52:2245
93. Schmidt E, Wiithrich N (1967) Helv Chim Acta 50:2058
94. Kolb DM, Przasnyski M, Gerischer H (1974) J Electroanal Chem 54:25
95. Gerischer H, Kolb DM, Przasnyski M (1974) Surf Sci 43:662
96. Vijh AK (1974) Surf Sci 46:282
97. Vetter KJ, Schultze JW (1972) Ber Bunsenges Phys Chem 76:920
98. Vetter KJ, Schultze JW (1972) Ber Bunsenoes Phys Chem 76:927
99. Schultze JW, Vetter KJ (1973) J Electroanal Chem 44:63
100. Lorenz WJ, Salié G (1977) J Electroanal Chem 80:1
101. Bewick A, Thomas B (1975) J Electroanal Chem 65:911
102. Bewick A, Thomas B (1976) J Electroanal Chem 70:239
103. Bewick A, Thomas B (1977) J Electroanal Chem 84:127
104. Bewick A, Jovićević JN, Thomas B (1977) Trans Faraday Disc 12:24
105. Rawlings KJ, Gibson MJ, Dobson PJ (1978) J Phys D 11:2059
106. Dickertmann D, Schultze WJ (1977) Electrochim Acta 22:117
107. Schultze JW, Dickertmann D (1976) Surf Sci 54:489
108. Dickertmann D, Koppitz FD, Schultze JW (1976) Electrochim Acta 21:967
109. Siegenthaler H, Jüttner K (1979) Electrochim Acta 24:109
110. Siegenthaler H, Jüttner K, Schmidt E, Lorenz WJ (1978) Electrochim Acta 23:1009
111. Jüttner K, Siegenthaler H (1978) Electrochim Acta 23:971
112. Staikov G, Jüttner K, Lorenz WJ, Budevski E (1978) Electrochim Acta 23:319
113. Staikov G, Jüttner K, Lorenz WJ, Schmidt E (1978) Electrochim Acta 23:305
114. Beckmann HO, Gerischer H, Kolb DM, Lehmpfuhl G (1977) Faraday Symp Chem Soc 12:51
115. Schultze JW, Dickertmann D (1977) Faraday Symp Chem Soc 12:36
116. Bewick A, Jovicevic J, Thomas B (1977) Faraday Symp Chem Soc 12:24
117. Herrmann HD, Wiithrich N, Lorenz WJ, Schmidt E (1976) J Electroanal Chem 68:289
118. Hilbert F, Mayer C, Lorenz WJ (1973) J Electroanal Chem 47:167
119. Jüttner K, Staikov G, Lorenz WJ, Schmidt E (1977) J Electroanal Chem 80:67
120. Schultze JW, Dickertmann D (1978) Ber Bunsenges Phys Chem 82:528
121. Horkans J, Cahan BD, Yeager E (1975) J Electrochem Soc 122:1585
122. Adzic RR, Yeager E, Cahan BD (1974) J Electrochem Soc 121:474
123. McIntyre JDE, Kolb DM (1970) Symp Faraday Soc 4:99
124. Lorenz WJ, Schmidt E, Staikov G, Bort H (1977) Faraday Symp Chem Soc 12:14
125. Bewick A, Thomas B (1977) J Electroanal Chem 85:329
126. Lorenz WJ, Herrmann HD, Wuthrich N, Hilbert F (1974) J Electrochem Soc 121:1167
127. Bort H, Jüttner K, Lorenz WJ, Schmidt E (1978) J Electroanal Chem 90:413

Chapter 2
Experimental Techniques and Structure of the Underpotential Deposition Phase

2.1 Introduction

The electrochemical deposition of metals on foreign substrates is a complex process, which includes a number of phase formation phenomena. The very initial electrodeposition stages of a metal, M, on a foreign substrate, S, involve adsorption reactions as well as two-dimensional (2D) and/or three-dimensional (3D) nucleation and growth processes. The most important factors determining the mechanism of electrochemical M phase formation on S are the binding energy between the metal adatoms (M_{ads}) and S, as well as the crystallographic misfit between the 3D M bulk lattice parameters and S. As we have shown in Fig. 1.3, when the binding energy between the depositing M-adatoms and the substrate atoms exceeds that between the atoms of the deposited metal, low dimensional iD metal phases ($i = 0$, 1 and 2) are formed onto the foreign metal substrate. This phenomenon, introduced in Chap. 1 as underpotential deposition (upd) [1–4], has been known for a long time and it has been intensively subject of study in the past decades since the 1970s. This has been demonstrated by many studies of the upd process of different metals on mono- and polycrystalline substrates as well as reviews on the subject. The understanding of the nature of this phenomenon as conceived in the middle 1990s can be found in the book of Lorenz et al. [1]. Reviews available in the literature include the works of Kolb et al., Abruña et al., Sudha and Sangaranarayanan, Aramata [5–8], and the work of Szabó [3] concerning the theoretical aspects of upd, updated by Leiva [9], and also the works of Adžic [10] and Kokkinidis [11], concerning mainly the catalytic effects of upd adatoms.

Monolayer amounts of metal adatoms obtained by upd alter the electronic properties of the substrate material itself by changing the interfacial reactivity, and therefore these systems have been the subject of a large number of studies, not only in terms of their fundamental aspects related to electrochemical phenomena (adsorption, charge transfer, nucleation and growth) but also in their technological application for corrosion inhibition or as models for the design of new electrocatalysts, between others. In addition, the study and applications of upd

O.A. Oviedo et al., *Underpotential Deposition*, Monographs in Electrochemistry,
DOI 10.1007/978-3-319-24394-8_2

processes involve now numerous disciplines apart from electrochemistry, such as chemistry, physics and materials science, as discussed in the remaining of this book.

Many electrochemical and surface characterization methods have been employed to study the upd phenomenon. Whereas electrochemical techniques provide valuable information on the kinetics and mechanisms of processes occurring at the metal/solution interface, the molecular specificity required to give unequivocal identification of species formed at electrode surfaces are obtained by a number of in situ and ex situ spectroscopies. These spectroscopic methods have been applied to augment electrochemical approaches and provide information on the elemental and molecular composition, the atomic geometry, and the electronic structure of the interface. The great progress that has been made in the development of new in-situ techniques allowed to obtain important information on electrode processes at the molecular and atomic level. In this Chapter, different techniques used for characterization of upd layers will be discussed briefly and illustrated by appropriate, representative examples.

2.2 Cyclic Voltammetry

Cyclic voltammetry has been and still is the most important routine method for characterizing the upd of a metal M on a foreign metal substrate. This technique consists of scanning linearly the potential of a stationary working electrode with a constant scan rate (dE/dt) between two chosen limits, one or more times, while the current is continuously monitored. The obtained cyclic current-potential curves offer a rapid location of redox potentials of electroactive species and provide a convenient evaluation of the effect of media upon the redox process. Any reaction at the electrode surface will usually be detected as a current superimposed to the base current due to double-layer charging.

The upd process is reflected in cathodic and anodic current density peaks at different potentials, indicating the deposition and dissolution of the metal adsorbate, respectively. The occurrence of distinct adsorption peaks in the cyclic voltammetric measurements indicates that the formation of 1–2 monolayers at underpotentials takes place in several energetically different adsorption steps.[1] The peak structure is found to depend strongly on the crystallographic orientation of the substrate and the density of crystals imperfections [1]. The number of these peaks and positions also depend on the substrate and the crystal plane on which the adsorption takes place as well as on the nature of the electrolyte. The peaks are not well-pronounced for polycrystalline electrodes whose surface presents different

[1] To learn more on the relationship between the peak potential and the energetic properties of the monolayer see Chap. 3.